Mitogenic Signaling Mediated by Oxidants in Ras-Transformed Fibroblasts

Kaikobad Irani, Yong Xia, Jay L. Zweier, Steven J. Sollott, Channing J. Der, Eric R. Fearon, Maitrayee Sundaresan, Toren Finkel, Pascal J. Goldschmidt-Clermont*

NIH 3T3 fibroblasts stably transformed with a constitutively active isoform of $p21^{Ras}$, $H\text{-}Ras^{V12}$ (v-H-Ras or EJ-Ras), produced large amounts of the reactive oxygen species superoxide ($\cdot O_2^-$). $\cdot O_2^-$ production was suppressed by the expression of dominant negative isoforms of Ras or Rac1, as well as by treatment with a farnesyltransferase inhibitor or with diphenylene iodonium, a flavoprotein inhibitor. The mitogenic activity of cells expressing $H\text{-}Ras^{V12}$ was inhibited by treatment with the chemical antioxidant *N*-acetyl-L-cysteine. Mitogen-activated protein kinase (MAPK) activity was decreased and c-Jun N-terminal kinase (JNK) was not activated in $H\text{-}Ras^{V12}$–transformed cells. Thus, $H\text{-}Ras^{V12}$–induced transformation can lead to the production of $\cdot O_2^-$ through one or more pathways involving a flavoprotein and Rac1. The implication of a reactive oxygen species, probably $\cdot O_2^-$, as a mediator of Ras-induced cell cycle progression independent of MAPK and JNK suggests a possible mechanism for the effects of antioxidants against *Ras-induced cellular transformation.*

Reactive oxygen species (ROS) have been conventionally regarded as having carcinogenic potential and have been associated with tumor promotion (*1*). Some tumor cells produce ROS (*2*), although the source of these products and their contribution to the transformed phenotype is not known. Certain ROS have also been shown to act as essential intracellular second messengers for several cytokines and growth factors (*3*). Thus, antioxidants may be protective against cancer and may inhibit cell proliferation, and intracellular ROS scavengers may actually contribute to suppression of the transformed phenotype (*4*).

The intracellular pathways leading to the generation of ROS are best characterized in phagocytic cells. In these specialized cells, the superoxide free radical ($\cdot O_2^-$) is generated by the multimolecular β-nicotinamide adenine dinucleotide phosphate (NADPH)–oxidase complex, which includes Rac, a member of the Ras superfamily of small guanosine triphosphate–binding proteins (*5*). In nonphagocytic cells, the proteins responsible for producing $\cdot O_2^-$ and other ROS are less well characterized, but they may be functionally similar to those involved in the phagocyte NADPH-oxidase complex (*6*).

The proto-oncogene $p21^{Ras}$ (c-Ras) itself participates in various cellular processes, including proliferation, differentiation, and cytoskeletal organization. Overexpression of Ras and mutations of Ras that render it constitutively active have been described in various human tumors (*7*). The signal transduction pathway by which Ras causes transformation includes Rac1 (*8*). However, the mechanisms and second messengers through which oncogenic Ras affects downstream targets are not fully understood. Because Rac1 can induce production of ROS in nonphagocytic cells (*9*), we investigated whether Ras-transformed cells also produce ROS through a pathway involving Rac1, and if so, whether ROS contribute to generation of the oncogenic phenotype.

We studied Ras-transformed NIH 3T3 fibroblasts stably expressing the $H\text{-}Ras^{V12}$ oncogene (*10*). A prototypical clonal cell line, A6, which has been extensively characterized and stably expresses $H\text{-}Ras^{V12}$ (*10*), was compared with Neo (a pool of control clonal lines not expressing oncogenic Ras) and with a clonal line of NIH 3T3 fibroblasts stably transformed with a constitutively active isoform of the protein kinase Raf (*11*), a downstream effector of Ras. We used electron paramagnetic resonance (EPR) spectroscopy and the spin trap 5,5-dimethyl-1-pyrroline-*N*-oxide (DMPO) to demonstrate that A6 cells displayed a 1:2:2:1 quartet signal (with $a_H = a_N = 14.9$ G) indicative of the DMPO-OH adduct, whereas Neo control cells and Raf-transformed cells did not generate such a signal (Fig. 1, A, B, and J). A similar, though weaker, signal was observed in another Ras-transformed clonal cell line, A2 (Fig. 1K) (*10*). The DMPO-OH adduct can be formed either by direct trapping of the hydroxyl radical (·OH) or by rapid breakdown of DMPO-OOH, the adduct formed by $\cdot O_2^-$ (*12*). Superoxide dismutase (SOD) quenched the observed signal, whereas catalase had no effect (Fig. 1, C and D). Although this result showed that the observed signal was attributable to $\cdot O_2^-$ trapping rather than to ·OH derived from H_2O_2, it did not rule out the possibility that H_2O_2 is generated within these cells, probably by the rapid dismutation of $\cdot O_2^-$. Small amounts of $\cdot O_2^-$, undetectable by EPR, might also be present within Neo and Raf-transformed cells. Production of $\cdot O_2^-$ by A6 cells was con-

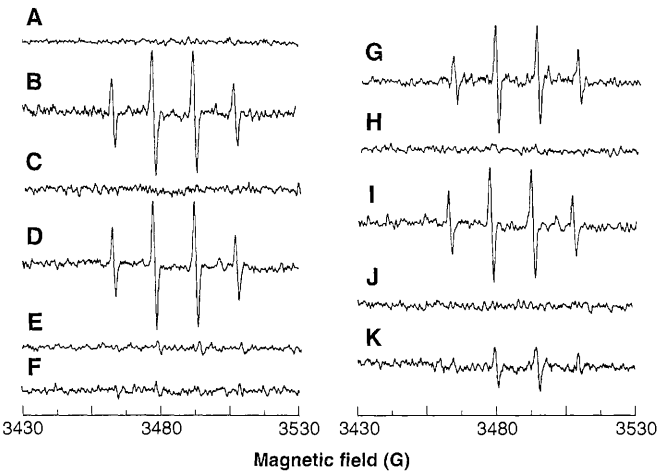

Fig. 1. Spin trapping and EPR spectroscopy. EPR spectra of A6, Neo, and Raf-transformed cells (untreated, treated as indicated, or transiently transfected as indicated) were recorded with the spin trap DMPO on 5×10^6 cells with a Bruker-IBM ER 300 spectrometer (*22*). (**A**) Neo; (**B**) A6; (**C**) A6 + Cu-Zn SOD (200 U/ml); (**D**) A6 + catalase (300 U/ml); (**E**) A6 + FPTase inhibitor (2 μM); (**F**) A6 + DPI (20 μM); (**G**) Neo + pEXVracV12 (*23*); (**H**) A6 + NAC (20 mM); (**I**) A6 + rotenone (50 μM); (**J**) Raf-transformed cells; and (**K**) A2. All measurements were in duplicate and were reproduced at least twice.

K. Irani, Y. Xia, J. L. Zweier, S. J. Sollott, Division of Cardiology, Department of Medicine, Johns Hopkins University School of Medicine, Baltimore, MD 21205, USA.
C. J. Der, Department of Pharmacology, University of North Carolina at Chapel Hill, Chapel Hill, NC 27599, USA.
E. R. Fearon, University of Michigan Medical Center, Ann Arbor, MI 48109, USA.
M. Sundaresan and T. Finkel, Cardiology Branch, National Heart, Lung, and Blood Institute, National Institutes of Health, Bethesda, MD 20892, USA.
P. J. Goldschmidt-Clermont, Division of Cardiology, Department of Medicine, and Department of Cell Biology and Anatomy, Johns Hopkins University School of Medicine, Baltimore, MD 21205, USA.

*To whom correspondence should be addressed at Heart and Lung Institute, Ohio State University, Columbus, OH 43210, USA.

firmed by a lucigenin-enhanced chemiluminescence (LUCL) assay, which has specificity for $\cdot O_2^-$ (*13*). A6 cells had a significantly stronger signal by LUCL assay relative to that of Neo cells (Student's *t* test, $P < 0.05$) (Fig. 2).

A6 cells transiently transfected with an expression plasmid encoding a dominant negative isoform of Ras, Ras^{N17}, showed a significantly weaker LUCL signal than that from cells transfected with the empty plasmid (Student's *t* test, $P < 0.05$) (Fig. 2). In addition, A6 cells treated with an inhibitor of farnesyl protein transferase (FPTase), which inhibits Ras-dependent transformation and results in morphological reversion of Ras-transformed cells (*14*), displayed an attenuation of the DMPO-OH signal (Fig. 1E); this observation showed that $\cdot O_2^-$ production in A6 cells is dependent on oncogenic Ras.

In phagocytic cells, production of $\cdot O_2^-$ during the microbiocidal oxidative burst requires the assembly of the flavoprotein-containing NADPH-oxidase complex. To determine whether a functionally similar enzyme was involved in the generation of $\cdot O_2^-$ by A6 cells, we treated A6 cells with diphenylene iodonium (DPI), a potent and highly selective flavoprotein inhibitor. The DMPO-OH signal was diminished in DPI-treated A6 cells (Fig. 1F). Treatment of A6 cells with rotenone, a mitochondrial oxidase inhibitor, did not reduce the EPR signal (Fig. 1I), which indicated that such oxidases have no role in generating the DMPO-OH signal.

The widely expressed Rac1 protein and the more selectively expressed Rac2 protein regulate production of ROS by phagocytic and nonphagocytic cells (*6*, *9*). Rac1 is believed to act downstream of Ras in mediating many cellular processes, and in certain cells it is essential for Ras-induced transformation (*8*, *15*). We therefore attempted to characterize the role of Rac1 in producing $\cdot O_2^-$ in Ras-transformed cells. Neo cells transiently transfected with an expression vector encoding $Rac1^{V12}$, a constitutively active mutant of Rac1, produced a DMPO-OH signal similar to that observed in A6 cells (Fig. 1G). Neo cells transfected with the vector with no cDNA insert produced no signal. A LUCL assay of A6 cells transiently expressing $Rac1^{N17}$, a dominant negative allele of Rac1, showed a reduction in $\cdot O_2^-$ production relative to that from A6 cells transiently transfected with the empty vector (Fig. 2). Expression of the $Rac1^{N17}$ mutant was confirmed by protein immunoblotting with an antibody to the myc epitope (9E10, Santa Cruz Biotechnology). These data strongly indicate that oncogenic Ras-transformed fibroblasts produce $\cdot O_2^-$ through a mechanism analogous to that of the NADPH-oxidase complex in phagocytes, which is dependent on Rac1.

From these results, we concluded that Ras transformation by overexpression of oncogenic Ras leads to the production of $\cdot O_2^-$. However, the functional significance of $\cdot O_2^-$ generation for the Ras-induced transformed phenotype was not known. A hallmark of Ras-transformed cells is their ability to progress through the cell cycle even under conditions of confluence and growth factor deprivation. A6 and Raf-transformed cells displayed a greater rate of DNA synthesis than did Neo cells under serum-starved conditions (Fig. 3A). To test whether $\cdot O_2^-$, or $\cdot O_2^-$-derived ROS, mediated this oncogenic Ras-induced mitogenic response, we treated A6 cells with the membrane-permeant antioxidant *N*-acetyl-L-cysteine (NAC). NAC effectively inhibited DNA synthesis in A6 cells in a dose-dependent manner (Fig. 3B). Likewise, there was a dose-dependent decrease in the DMPO-OH signal in A6 cells treated with NAC (Fig. 3C). Complete inhibition of the DMPO-OH signal by NAC did not result in a reduction of DNA synthesis to an amount comparable to that in Neo cells, which

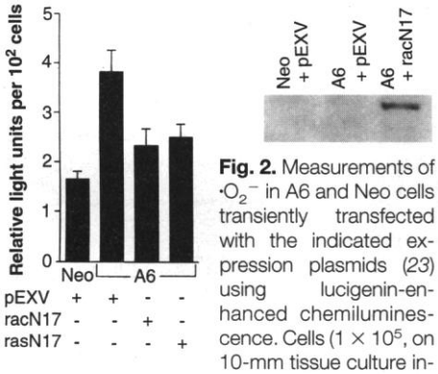

Fig. 2. Measurements of $\cdot O_2^-$ in A6 and Neo cells transiently transfected with the indicated expression plasmids (*23*) using lucigenin-enhanced chemiluminescence. Cells (1×10^5, on 10-mm tissue culture inserts) were placed in 0.25 mM lucigenin in Krebs-Hepes buffer, and the luminescent signal was recorded immediately thereafter for 1 min with a Monolight 2010 luminometer. Background luminescence from blank inserts was subtracted. Values from a representative experiment are expressed as mean relative light units per 10^5 cells ± SEM.

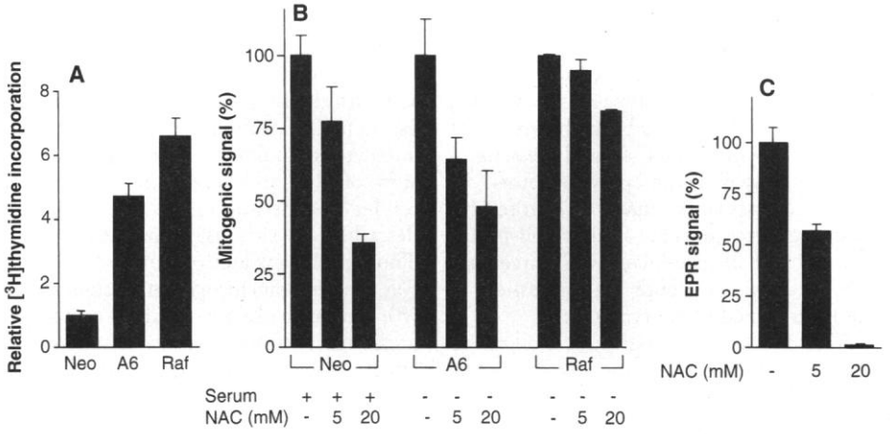

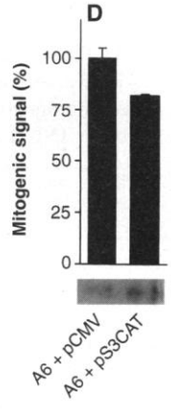

Fig. 3. Effect of ROS on cell division. (**A**) Relative [³H]thymidine incorporation in serum-starved A6, Neo, and Raf-transformed cells (*24*). Serum-starved cells were incubated with [³H]thymidine (1 μCi/ml) for 4 hours, and radioactivity in trichloroacetic acid (TCA)–precipitable material was measured. Values were obtained from triplicate wells and are expressed as mean ± SEM relative to Neo cells. (**B**) Inhibition of mitogenic signaling in A6, Neo, and Raf-transformed cells. Serum-starved or serum-stimulated cells were treated for 4 hours with the indicated concentrations of NAC and incubated with [³H]thymidine (1 μCi/ml) for 4 hours. Radioactivity from TCA-precipitable material was measured; values are expressed as percent of mitogenic signal of untreated cells and represent the mean ± SEM from triplicate wells. (**C**) Reduction in EPR signal of A6 cells treated with NAC. EPR spectra of untreated cells or cells treated with the indicated concentration of NAC for 20 min were obtained. Values are expressed as percent of signal magnitude of untreated cells and represent mean ± SEM of duplicate measurements. (**D**) Effect of catalase overexpression on the mitogenic signal of A6 cells. A6 cells were transiently transfected with an empty plasmid or with an expression plasmid for human catalase (*21*) and 48 hours later they were incubated with [³H]thymidine (1 μCi/ml) for 4 hours. Radioactivity from TCA-precipitable material was measured; values are expressed as percent of mitogenic signal of cells transfected with the empty plasmid and represent the mean ± SEM from duplicate wells. Expression of catalase was determined in 20 μg of total cell lysates from A6 cells transfected with the indicated plasmids (*23*). Extracts were subjected to immunoblotting with an antibody to human catalase (CalBiochem) (*25*).

suggested that $\cdot O_2^-$ may not be the sole mediator of mitogenic signaling within Ras-transformed A6 cells. The inhibition of DNA synthesis with addition of NAC was small in Raf-transformed cells (Fig. 3B); this finding implies that Raf-induced mitogenic signaling is much less dependent on the production of ROS, and it is consistent with the finding that Raf-induced transformation is independent of Rac1 (*8*). Serum-stimulated Neo cells treated with NAC also showed a dose-dependent decrease in DNA synthesis (Fig. 3B), supporting the role of Ras-mediated ROS production in serum-induced mitogenic signaling (*16*). The viability of A6, Neo, and Raf-transformed cells treated with NAC was not affected, as judged by trypan blue exclusion (*17*).

By altering the intracellular redox milieu, NAC could be suppressing mitogenic signaling mediated through ROS other than $\cdot O_2^-$. Therefore, we transiently transfected A6 cells with an empty plasmid and an expression plasmid encoding human catalase. Overexpression of catalase resulted in a decrease of 15 to 20% in DNA synthesis in A6 cells (Fig. 3D), thus implicating H_2O_2, a product of $\cdot O_2^-$, as another (though less important) potential mediator of mitogenic signaling in Ras-transformed cells. Both $\cdot O_2^-$ and H_2O_2 have been implicated in the proliferation of transformed and nontransformed cells (*4*).

Members of the mitogen-activated protein kinase (MAPK) family of proteins are effectors of the Ras-Raf pathway and can be phosphorylated and activated in response to various extracellular signals (*18*). In certain cells, MAPK activation in response to growth factors is dependent on the production of ROS (*3*). MAPKs in turn act to phosphorylate and activate certain nuclear transcription factors (*19*). We therefore investigated whether MAPK activity was up-regulated by $\cdot O_2^-$ in A6 cells. Relative to Neo cells, A6 cells under serum-starved conditions had decreased amounts of p44 and p42 MAPK tyrosine phosphorylation (Fig. 4A) and MAPK activity (*17*). As expected, p44 and p42 MAPK were activated in the Raf-transformed cells (Fig. 4A). Amounts of MAPK were equivalent in all cell lines (*17*). We conclude that $\cdot O_2^-$ does not lead to MAPK activation in A6 cells, and that the mitogenic activity of these cells is mediated through a MAPK-independent pathway.

c-Jun N-terminal kinase (JNK) can also induce transcriptional activity through phosphorylation and activation of c-Jun. Ras and Rac1 modulate JNK activity (*20*). JNK activity was comparably low in both Neo and A6 cells (Fig. 4B). In addition, JNK activity that was increased in both cells in response to tumor necrosis factor–α (TNF-α) was blunted if the cells were first treated with NAC (Fig. 4D). H-Ras^{V12}–induced $\cdot O_2^-$ production by A6 cells therefore does not up-regulate JNK activity, but JNK activity in these cells seems to be sensitive to alterations of the intracellular redox state.

Unlike transient elevations in intracellular ROS that occur in response to extracellular stimuli in plant and animal cells (*3*), we observed constitutive production of ROS in cell lines transformed by overexpression of oncogenic Ras. The ROS produced constitutively by A6 cells appear to function differently from the burst of ROS generated by growth factors that activate the Ras pathway. The decreased activation of the MAPK pathway in A6 cells is contrary to observations with growth factor–induced ROS production or transient expression of oncogenic Ras in nontransformed cells (*3*, *20*). Although increased tyrosine kinase activity occurs after addition of growth factors or high concentrations of exogenous ROS in various cells, including NIH 3T3 cells (*3*), the A6 cells exhibited reduced tyrosine kinase activity of key signaling molecules such as the platelet-derived growth factor receptor (*10*, *17*). Finally, JNK activity, though seemingly sensitive to the redox state of the cell, was not enhanced in the Ras-transformed cells, whereas transient expression of oncogenic Ras in nontransformed cells leads to activation of JNK (*20*).

We therefore propose that constitutive production of ROS in Ras-transformed A6 cells activates intracellular pathways that may be distinct from those that are activated by extracellular growth factors. In our model of H-Ras^{V12}–transformed NIH 3T3 cells, production of ROS correlates with the ability of these cells to progress through the cell cycle in the absence of growth factors. This phenomenon suggests that modulation of the redox state of the cell may provide one mechanism to explain the observation that some antioxidants appear to exert protective effects against human cancers.

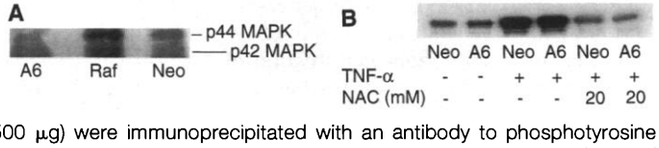

Fig. 4. (**A**) Tyrosine phosphorylation of p42 and p44 MAPK in serum-starved A6, Neo, and Raf-transformed cells. Total cell lysates (500 μg) were immunoprecipitated with an antibody to phosphotyrosine (4G10, UBI) and immunoprecipitates were probed with an antibody to the p42 and p44 isoforms of MAPK (erk1-CT, UBI) (*25*). (**B**) JNK enzymatic activity in A6 and Neo cells and the effect of NAC on TNF-α–stimulated JNK activity. Equal amounts of protein from extracts of serum-starved A6 and Neo cells treated as indicated [NAC for 12 hours, TNF-α for 15 min] were precipitated with agarose-conjugated human c-Jun(1–169)–GST (UBI). Solid-phase kinase assays were done on the precipitates as described (*26*). Phosphorylated proteins were eluted with Laemmli buffer, resolved by SDS-PAGE, and autoradiographed.

REFERENCES AND NOTES

1. B. N. Ames, *IARC Sci. Publ.* **89**, 407 (1988).
2. T. P. Szatrowski and C. F. Nathan, *Cancer Res.* **51**, 794 (1991).
3. M. Sundaresan, Z.-X. Yu, V. J. Ferrans, K. Irani, T. Finkel, *Science* **270**, 296 (1995); M. Ohba, M. Shibanuma, T. Kuroki, K. Nose, *J. Cell Biol.* **126**, 1079 (1994); B. Meier *et al.*, *Biochem. J.* **263**, 539 (1989); Y. Y. C. Lo and T. F. Cruz, *J. Biol. Chem.* **270**, 11727 (1995); A. Levine, R. Tenhaken, R. Dixon, C. Lamb, *Cell* **79**, 583 (1994); G. B. Bulkley, *Lancet* **344**, 934 (1994).
4. M. Rautalahti and J. Huttunen, *Ann. Med.* **25**, 435 (1993); R. H. Burdon, V. Gill, D. Alliangana, *Free Radical Res. Comm.* **24**, 81 (1996); R. H. Burdon and V. Gill, *ibid.* **19**, 203 (1993); S. L. Church *et al.*, *Proc. Natl. Acad. Sci. U.S.A.* **90**, 3113 (1993).
5. D. Diekmann, A. Abo, C. Johnston, A. W. Segal, A. Hall, *Science* **265**, 531 (1994); G. M. Bokoch, *Curr. Opin. Cell Biol.* **6**, 212 (1994); P. G. Heyworth *et al.*, *Mol. Biol. Cell* **4**, 1217 (1993); U. G. Knaus *et al.*, *J. Biol. Chem.* **267**, 23575 (1992); U. G. Knaus, P. G. Heyworth, T. Evans, J. T. Curnutte, G. M. Bokoch, *Science* **254**, 1512 (1991); A. Abo *et al.*, *Nature* **353**, 668 (1991); T. Mizuno *et al.*, *J. Biol. Chem.* **267**, 10215 (1992).
6. B. Meier, A. R. Cross, J. T. Hancock, F. J. Kaup, O. T. G. Jones, *Biochem. J.* **275**, 241 (1991); B. Meier, A. J. Jesaitis, A. Emmendorfer, J. Roesler, M. T. Quinn, *ibid.* **289**, 481 (1993); H. I. Krieger-Brauer and H. Kather, *ibid.* **307**, 549 (1995).
7. M. Barbacid, *Annu. Rev. Biochem.* **56**, 779 (1987); J. L. Bos, *Cancer Res.* **49**, 4682 (1989).
8. R. Qiu, J. Chen, D. Kim, F. McCormick, M. Symons, *Nature* **374**, 457 (1995).
9. M. Sundaresan *et al.*, *Biochem. J.* **318**, 379 (1996).
10. A. W. Heldman *et al.*, *Circ. Res.* **78**, 312 (1996).
11. S. M. Oldham, G. J. Clark, L. M. Gangarosa, R. J. Coffey Jr., C. J. Der, *Proc. Natl. Acad. Sci. U.S.A.* **93**, 6924 (1996).
12. J. L. Zweier *et al.*, *J. Biol. Chem.* **269**, 24156 (1994).
13. H. Gyllenhammar, *J. Immunol. Methods* **97**, 209 (1987).
14. N. E. Kohl *et al.*, *Science* **260**, 1934 (1993); G. C. Pendergast *et al.*, *Mol. Cell. Biol.* **14**, 4193 (1994).
15. A. J. Ridley, H. F. Paterson, C. L. Johnston, D. Diekmann, A. Hall, *Cell* **70**, 401 (1992); C. D. Nobes and A. Hall, *ibid.* **81**, 53 (1995); A. J. Ridley and A. Hall, *ibid.* **70**, 389 (1992).
16. L. S. Mulcahy, M. R. Smith, D. W. Stacey, *Nature* **313**, 241 (1985); H. Cai, J. Szeberenyl, G. M. Cooper, *Mol. Cell. Biol.* **10**, 5314 (1990).
17. K. Irani and P. J. Goldschmidt-Clermont, unpublished observations.
18. M. H. Cobb, T. G. Boulton, D. J. Robbins, *Cell Regul.* **2**, 965 (1991); C. M. Crews and R. L. Erickson, *Cell* **74**, 215 (1993).
19. B. J. Pulverer *et al.*, *Nature* **353**, 670 (1991); H. Gille, A. D. Sharrocks, P. E. Shaw, *ibid.* **358**, 414 (1992).
20. A. Minden *et al.*, *Cell* **81**, 1147 (1995); O. A. Coso *et al.*, *ibid.*, p. 1137; J. K. Westwick *et al.*, *Proc. Natl. Acad. Sci. U.S.A.* **91**, 6030 (1994); M. F. Olson, A. Ashworth, A. Hall, *Science* **269**, 1270 (1995).
21. S. C. Erzurum, P. Lemarchand, M. A. Rosenfeld, J. Yoo, R. G. Crystal, *Nucleic Acids Res.* **21**, 1607 (1993).
22. The spin trap DMPO (Aldrich, >97% pure) was used

at 50 mM with the spectrometer set at a microwave frequency of 9.77 GHz with 20 mW of microwave power and a modulation amplitude of 0.5 G. Treatment with Cu-Zn SOD (Sigma), catalase (Sigma), DPI (Toronto Research), or *N*-acetyl-L-cysteine (Sigma) was for 20 min before recording of EPR spectra. Treatment with the FPTase inhibitor H-Ampamb-Phe-Met-OH (LC Laboratories) was for 48 hours before obtaining spectra. At this concentration and with this duration of treatment, no cellular toxicity was observed.

23. The empty expression plasmid pEXV and the expression plasmids pEXVracV12 (encoding myc epitope–tagged constitutively active Rac1), pEXVracN17 (dominant negative Rac1), pCMVrasN17 (dominant negative Ras), and pS3CAT (catalase) have been described (*15, 21*). Transient transfections were done according to the manufacturer's recommendations using 15 μl of Lipofectamine (Gibco) and 5 μg of DNA per 10^5 cells. EPR spectra were obtained 48 hours after transfection. For the LUCL assay, 1×10^5 transfected cells were replated onto each tissue culture insert 24 hours after transfection and the assay was performed 24 hours later. Protein immunoblot analysis was done on cells 48 hours after transfection.
24. Established A6, Neo, and Raf-transformed cell lines (*10, 11*) were maintained in Dulbecco's modified Eagle's medium with 10% fetal bovine serum (Gibco) and G418 (250 μg/ml, Sigma). Expression of H-Ras^{V12} in A6 cells was confirmed by protein immunoblotting with an antibody to H-Ras (Oncogene Science). Serum starvation was carried out in 0.1% serum for 48 hours.
25. For immunoprecipitation and protein immunoblotting, cells were harvested in complete lysis buffer [145 mM NaCl, 0.1 mM $MgCl_2$, 15 mM Hepes, 10 mM EGTA (pH 7.0), 0.1% Triton X-100, 20 μg/ml each of chymostatin, pepstatin, antipain, and leupeptin, 1 mM 4-(2-aminoethyl)benzylsulfonyl fluoride, and 1 mM Na orthovanadate]. Immunoprecipitates or total cell lysates were subjected to SDS–polyacrylamide gel electrophoresis (PAGE) and transferred to nitrocellulose filters. Blots were then probed with the indicated antibody and developed by ECL (Amersham).
26. M. Hibi *et al.*, *Genes Dev.* **7**, 2135 (1993).
27. We thank A. Hall for providing the plasmids encoding the Rac1 mutant isoforms, L. Feig for Ras^{N17} cDNA, S. Erzurum for human catalase cDNA, and C. Lowenstein, C. Dang, and A. Hoang for helpful criticisms. Supported by NIH grant HL52315 (P.J.G.-C. and J.L.Z.), an Established Investigator Award, American Heart Association (P.J.G.-C.), and the Bernard Foundation.

8 November 1996; accepted 29 January 1997

A Member of the Frizzled Protein Family Mediating Axis Induction by Wnt-5A

Xi He,*† Jean-Pierre Saint-Jeannet, Yanshu Wang, Jeremy Nathans, Igor Dawid, Harold Varmus

In *Xenopus laevis* embryos, the Wingless/Wnt-1 subclass of Wnt molecules induces axis duplication, whereas the Wnt-5A subclass does not. This difference could be explained by distinct signal transduction pathways or by a lack of one or more Wnt-5A receptors during axis formation. Wnt-5A induced axis duplication and an ectopic Spemann organizer in the presence of hFz5, a member of the Frizzled family of seven-transmembrane receptors. Wnt-5A/hFz5 signaling was antagonized by glycogen synthase kinase-3 and by the amino-terminal ectodomain of hFz5. These results identify hFz5 as a receptor for Wnt-5A.

The *Drosophila melanogaster* tissue polarity gene *frizzled* (*fz*), which encodes a receptor-type protein (Fz) with seven putative transmembrane helixes (*1*), belongs to a family of related genes found in *Caenorhabditis elegans*, *Drosophila*, zebrafish, chicken, and mammals (*2–4*). DFz2, a Fz-type protein from *Drosophila*, functions as a receptor for the Wingless (Wg) protein (*4*), a member of the Wnt family of secreted signaling molecules essential for animal development (*5*). Upon transfection of *Drosophila* tissue culture cells, DFz2 confers both the ability to bind Wg at the cell surface and Wg responsiveness, as measured by accumulation of Armadillo protein (*4*). Certain mammalian Fz proteins also confer the Wg binding property to transfected cells (*4*) and can enhance the localization of Wnt-8 to the plasma membrane in *Xenopus laevis* embryos (*6*). Thus, the fz gene family may encode receptors for Wnt molecules, but the scarcity of soluble Wnt proteins complicates the study of ligand-receptor interactions and their specificity. Therefore, we used the *Xenopus* embryo to assay for such interactions and their specificity.

Mouse Wnt-1, *Xenopus* wnt-3A (Xwnt-3A), Xwnt-8, and *Drosophila* Wg induce dorsal axis duplication when small amounts, usually 1 to 10 pg, of their corresponding RNAs are injected into the ventral side of early *Xenopus* embryos (*7*). In contrast, Xwnt-5A RNA fails to do so even after ventral injection at higher doses (75 pg to 1 ng per embryo); instead, dorsal injection of Xwnt-5A RNA generates head and tail defects that may result from perturbation of cell movements during gastrulation (*8*). Xwnt-4 and Xwnt-11 behave similarly to Xwnt-5A (*9*). The Xwnt-8 dorsalizing function is observed before the mid-blastula transition when zygotic transcription begins, whereas the Xwnt-5A effect occurs after mid-blastula transition (*7, 8, 10, 11*). The difference between the effects of Xwnt-8 and Xwnt-5A may reflect the activation of distinct signaling pathways (*11*) or the lack of one or more functional Xwnt-5A receptors during axis formation.

To examine whether a particular Fz protein can function as an Xwnt-5A receptor, synthetic RNAs corresponding to Dfz2 (*4*) and six mammalian fz cDNAs—mfz3, mfz4, mfz6, mfz7, mfz8 (from mouse), and hfz5 [from human (*3*)]—were pooled into two groups and coinjected with 10 pg of Xwnt-5A RNA into the ventral side of embryos at the four-cell stage (*12*). Injection of Xwnt-5A alone, either fz group alone, or Xwnt-5A together with fz group 2 (mfz3, mfz4, mfz6, and mfz7) produced no phenotypic effects (Fig. 1A). However, coinjection of Xwnt-5A with fz group 1 RNAs (Dfz2, hfz5, and mfz8) induced extensive dorsal axis duplication (Fig. 1A) (*13*); in many cases, duplication was complete, as determined by the presence of anterior structures such as the eyes and the cement gland. When the three fz RNAs in group 1 were individually tested, Xwnt-5A plus hfz5 generated similar degrees of axis duplication, whereas Xwnt-5A plus Dfz2 or mfz8 did not (Fig. 1B). Thus, hFz5 alone among the Fz proteins tested is responsible for mediating axis induction by Xwnt-5A. Dorsal injection of the same concentration of Xwnt-5A plus hfz5 RNAs produced no axis duplication and injected embryos appeared normal.

The mature Wnt-5A proteins (after cleavage of the signal peptides) are 100% identical between mouse and human, and 95% identical between mouse and *Xenopus* (*8, 14*). Given this high degree of sequence identity, it is not surprising that murine wnt-5A RNA (*15*) also induced axis duplication when coinjected with hfz5 RNA, albeit less efficiently (Fig. 1C). The lower efficiency might be due to effects of untranslated regions in the murine wnt-5A construct (*15*) on RNA stability or translation efficiency or both.

Axis duplication by Xwnt-5A plus fz group 1 or hfz5, as described above, was observed in 14 of 20 embryo batches tested

X. He and H. Varmus, National Cancer Institute, Building 49, Room 4A56, National Institutes of Health, Bethesda, MD 20892, USA.
J.-P. Saint-Jeannet and I. Dawid, National Institute of Child Health and Human Development, National Institutes of Health, Bethesda, MD 20892, USA.
Y. Wang and J. Nathans, Howard Hughes Medical Institute, Department of Molecular Biology and Genetics, The Johns Hopkins University School of Medicine, Baltimore, MD 21205, USA.

*Present address: Division of Neuroscience, Enders 379, Children's Hospital/Harvard Medical School, 300 Longwood Avenue, Boston, MA 02115, USA
†To whom correspondence should be addressed. E-mail: xhe@nhgri.nih.gov